Cold-Activated Lipid Dynamics in Adipose Tissue Highlights a Role for Cardiolipin in Thermogenic Metabolism

Lynes, Matthew D.; Shamsi, Farnaz; Sustarsic, Elahu Gosney; Leiria, Luiz O.; Wang, Chih Hao; Su, Sheng Chiang; Huang, Tian Lian; Gao, Fei; Narain, Niven R.; Chen, Emily Y.; Cypess, Aaron M.; Schulz, Tim J.; Gerhart-Hines, Zachary; Kiebish, Michael A.; Tseng, Yu Hua

Published in:
Cell Reports

DOI:
10.1016/j.celrep.2018.06.073

Publication date:
2018

Document version
Publisher's PDF, also known as Version of record

Resource

Cell Reports

Cold-Activated Lipid Dynamics in Adipose Tissue Highlights a Role for Cardiolipin in Thermogenic Metabolism

Graphical Abstract

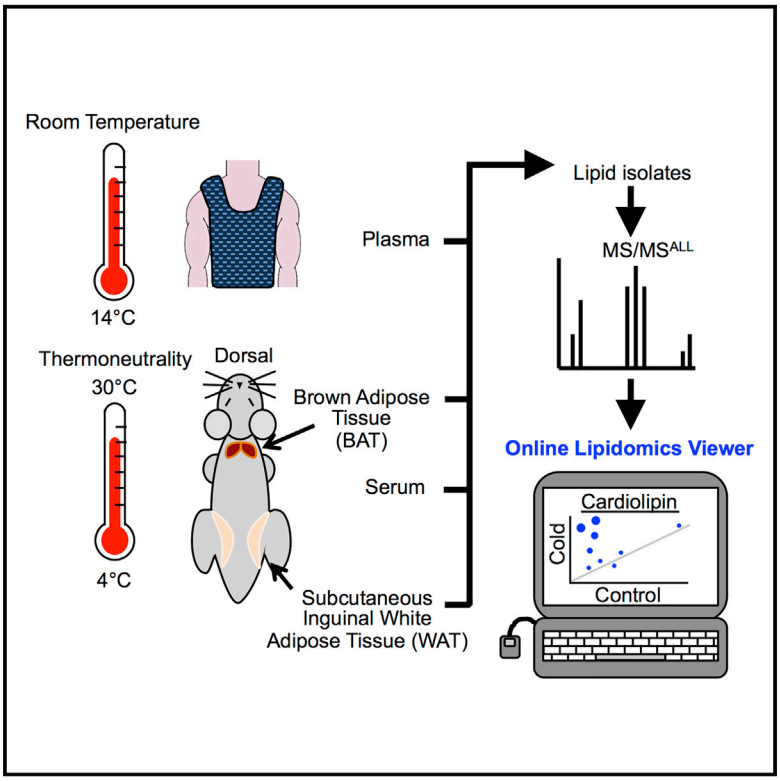

Authors

Matthew D. Lynes, Farnaz Shamsi, Elahu Gosney Sustarsic, ..., Zachary Gerhart-Hines, Michael A. Kiebish, Yu-Hua Tseng

Correspondence

yu-hua.tseng@joslin.harvard.edu

In Brief

In this resource, Lynes et al. use a sensitive MS/MS^{ALL} technique to profile over 1,000 lipid species in the blood and adipose tissue of humans and mice exposed to cold. Using the online viewer they created to view these data, pathways activated by cold exposure can be identified.

Highlights

- We report lipid profiles of cold-exposed humans and mice by MS/MS^{ALL} shotgun lipidomics
- We profiled circulating as well as brown and white adipose lipids in response to cold
- We identified a bio-signature of cardiolipin biogenesis in cold humans and mice
- We created an online tool to visualize changes of specific lipid species in our study

Lynes et al., 2018, Cell Reports *24*, 781–790
July 17, 2018
https://doi.org/10.1016/j.celrep.2018.06.073

CellPress

Cell Reports
Resource

Cold-Activated Lipid Dynamics in Adipose Tissue Highlights a Role for Cardiolipin in Thermogenic Metabolism

Matthew D. Lynes,[1] Farnaz Shamsi,[1] Elahu Gosney Sustarsic,[2] Luiz O. Leiria,[1] Chih-Hao Wang,[1] Sheng-Chiang Su,[1] Tian Lian Huang,[1] Fei Gao,[3] Niven R. Narain,[3] Emily Y. Chen,[3] Aaron M. Cypess,[4] Tim J. Schulz,[1,5] Zachary Gerhart-Hines,[2] Michael A. Kiebish,[3] and Yu-Hua Tseng[1,6,7,*]

[1]Section on Integrative Physiology and Metabolism, Joslin Diabetes Center, Harvard Medical School, Boston, MA 02215, USA
[2]The Novo Nordisk Foundation Center for Basic Metabolic Research, University of Copenhagen, Copenhagen, Denmark
[3]BERG, Framingham, MA 01701, USA
[4]NIH, Bethesda, MD 20814, USA
[5]German Institute of Human Nutrition, Potsdam-Rehbrücke, Germany
[6]Harvard Stem Cell Institute, Harvard University, Cambridge, MA 02138, USA
[7]Lead Contact
*Correspondence: yu-hua.tseng@joslin.harvard.edu
https://doi.org/10.1016/j.celrep.2018.06.073

SUMMARY

Thermogenic fat expends energy during cold for temperature homeostasis, and its activity regulates nutrient metabolism and insulin sensitivity. We measured cold-activated lipid landscapes in circulation and in adipose tissue by MS/MS^{ALL} shotgun lipidomics. We created an interactive online viewer to visualize the changes of specific lipid species in response to cold. In adipose tissue, among the approximately 1,600 lipid species profiled, we identified the biosynthetic pathway of the mitochondrial phospholipid cardiolipin as coordinately activated in brown and beige fat by cold in wild-type and transgenic mice with enhanced browning of white fat. Together, these data provide a comprehensive lipid bio-signature of thermogenic fat activation in circulation and tissue and suggest pathways regulated by cold exposure.

INTRODUCTION

Brown adipose tissue (BAT) functions in energy expenditure due, in part, to its role in temperature regulation, and its activity is inversely correlated to body mass index and percent body fat, making it an attractive target for anti-obesity therapies (Blondin et al., 2015; Cypess et al., 2012). Thermogenic adipocytes can also arise in white adipose tissue (WAT) through an inducible process called "browning," giving rise to brown-like cells, termed beige or brite adipocytes (Lynes and Tseng, 2018; Petrovic et al., 2010; Wu et al., 2012). This thermogenic capacity is mainly conferred by its unique expression of uncoupling protein 1 (UCP1) in the mitochondria, although UCP1-independent thermogenic mechanisms have recently been described (Kazak et al., 2015). UCP1 uncouples oxidative phosphorylation to generate heat (Cannon et al., 2006; Cinti, 2017; Lynes and Tseng, 2015). During cold exposure, the proton motive force used to produce heat in thermogenic adipocytes must be maintained through catabolism of metabolic substrates such as glucose and fatty acids (Seale et al., 2009). To resupply fuels for cold-induced energy expenditure, lipolysis is activated in WAT, and genetic blockade of adipose tissue lipolysis blocks BAT thermogenic function (Haemmerle et al., 2006; Schreiber et al., 2017), highlighting both the role of BAT lipolysis and the role of WAT as a fuel source for BAT during cold challenge. In addition to the high levels of glucose BAT takes up in response to cold (Chondronikola et al., 2014; Cooney et al., 1985; Orava et al., 2011), it also takes up lipid and cholesterol when activated (Bartelt et al., 2011, 2017; Berbée et al., 2015).

Recently, the extreme sensitivity of mass spectrometry has been leveraged to measure the concentration of many different lipid species from the same sample. In mice, these studies have demonstrated that the lipidomic profile of BAT and WAT are distinct (Hoene et al., 2014); further, cold induces selective remodeling of triacylglycerols (TAGS) and glycerophospholipids in BAT (Lu et al., 2017; Marcher et al., 2015). While these data are informative, a comprehensive database and tools for analyzing specific lipid species are still missing. In addition, although serum lipidomics from mice exposed to cold have recently been reported (Simcox et al., 2017), the circulating lipidome of humans exposed to cold exposure has been, thus far, limited to a small set of fewer than 100 oxidized lipid species (Lynes et al., 2017).

We report here a comprehensive untargeted analysis of the lipid composition of plasma from human subjects during cold challenge by tandem mass spectrometry (MS/MS)^{ALL} shotgun lipidomics. These data, comprising approximately 1,600 validated individual lipid species from 18 different lipid families, are available online in an easy-to-use viewer designed to allow researchers to analyze this data efficiently. In this dataset, as well as in lipidomic data from sera of mice housed in the

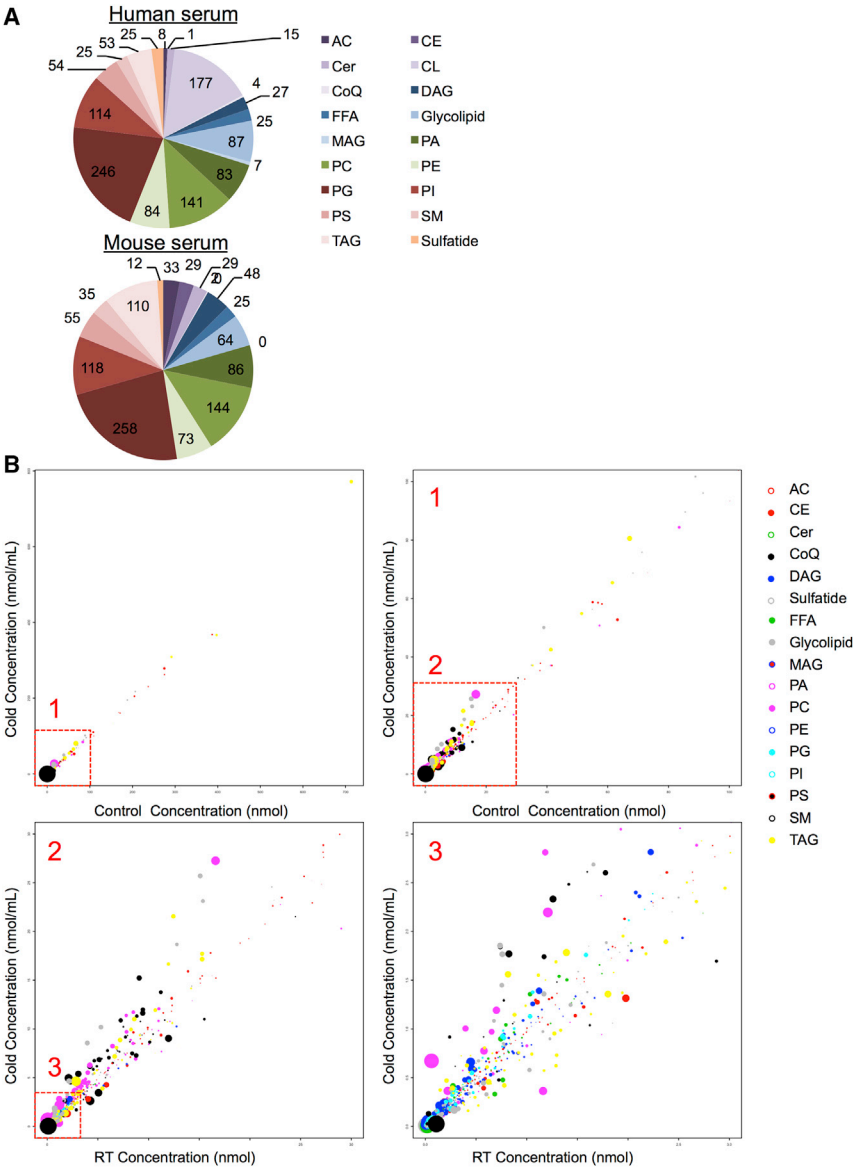

Figure 1. Identification of a Lipid Bio-signature of Cold Exposure in Mice and Humans

(A) Distribution of lipid classes that were considered for subsequent analysis in all samples detected by MS/MS^{ALL}. Lipid classes measured in circulation were: acyl-carnitine (AC), cholesterol ester (CE), ceramide (Cer), CoQ, diacylglycerol (DAG), free fatty acid (FFA), glycolipid (MonoHex and DiHex), phosphatidic acid (PA), phosphatidylcholine (PC), phosphatidylethanolamine (PE), phosphatidylglycerol (PG), phosphatidylinositol (PI), phosphatidylserine (PS), sphingomyelin (SM), triacylglycerol (TAG), and sulfatide. The number for each class denotes the number of species in that class that reached the level of detection in control (room temperature/thermoneutral) conditions.

(B) Concentration of lipids measured in human plasma in control samples (x axis) compared to cold-exposed samples (y axis). Data are means with smaller p values denoted by the larger circles. In the chart, the area in the red box corresponds to the chart with the same number in the top left corner. n = 9 subjects.

RESULTS

Circulating Lipid Profiles of Thermogenic Activation in Mice and Humans

To establish a comprehensive landscape of circulating lipids during cold challenge, we performed lipidomics on plasma or serum samples from cold-exposed mice and humans. We predicted over 2,300 different lipid species in both blood and tissue samples, consisting of almost 1,600 phospholipid species; more than 150 mono-, di-, and tri-acylglycerides; and 600 other lipid species and could detect approximately 70% of these lipids above background in at least one sample. As a threshold, we only analyzed lipids that were detectable above background in at least half of the samples, and we could robustly detect more than 1,000 of these lipids in circulation (Figure 1A). Lipid classes measured included: acyl-carnitine (AC), cholesterol ester (CE), ceramide (Cer), cardiolipin, coenzyme Q (CoQ), diacylglycerol (DAG), free fatty acid (FFA), glycolipid (MonoHex and DiHex), monoacylglycerol (MAG), phosphatidic acid (PA), phosphatidylcholine (PC), phosphatidylethanolamine (PE), phosphatidylglycerol (PG), phosphatidylinositol (PI), phosphatidylserine (PS), sphingomyelin (SM), sulfatide, and TAG. Sulfatides were only measured in circulation, while cardiolipin was only measured in tissue. We included the data for the concentration of each different species as supplements to this article (Tables S1, S2, and S3). To facilitate data analysis and visualization, we created a convenient and interactive viewer to provide the relative changes and associated false discovery rates (FDRs)

cold or at a thermoneutral temperature, we found coordinated increases of many phospholipids, especially phosphatidylglycerol. The circulating lipidome was consistent with increased concentrations of lipid metabolites in the cardiolipin (CL) biosynthetic pathway that we found by performing MS/MS^{ALL} on BAT and WAT from cold-exposed mice compared to tissue from mice housed in thermoneutral conditions. BAT cardiolipin metabolism is well known to be activated by cold exposure (Ogawa et al., 1987; Ricquier et al., 1978; Strunecká et al., 1981), and we found that this pathway was also increased in beige adipose tissue. Our databases can be used to generate hypotheses for the complex metabolic networks that are regulated by thermogenic fat activity in humans and rodents and support the evidence that cardiolipin metabolism in brown and beige fat plays a critical role in enhancing thermogenic function during cold challenge.

A

Lipid Species	Spearman Cor.[a]	p-value
Lyso-PG 18:0	0.72	0.0007476
CE 22:1	0.56	0.01626
PG 20:0/22:5	0.55	0.017
Lyso-PC O-22:0	0.55	0.01828
PA 18:0/18:0	0.55	0.01909
PE O-36:6	0.53	0.02421
Lyso-PG 18:1	0.50	0.03492
Glycolipid d18:1/24:0	-0.72	0.0007673
PE 38:7 /PE O-38:0	-0.64	0.003883
DAG 34:0	-0.58	0.0116
DAG 34:3	-0.54	0.02199
DAG 32:1	-0.53	0.02229
Glycolipid d18:1/14:1	-0.52	0.02556
PS 16:0/16:1	-0.51	0.03075
Glycolipid d18:1/22:2	-0.50	0.03363
PS 18:1/20:2	-0.50	0.03449
Glycolipid d18:2/16:0	-0.50	0.03536

[a]Spearman correlation coefficient

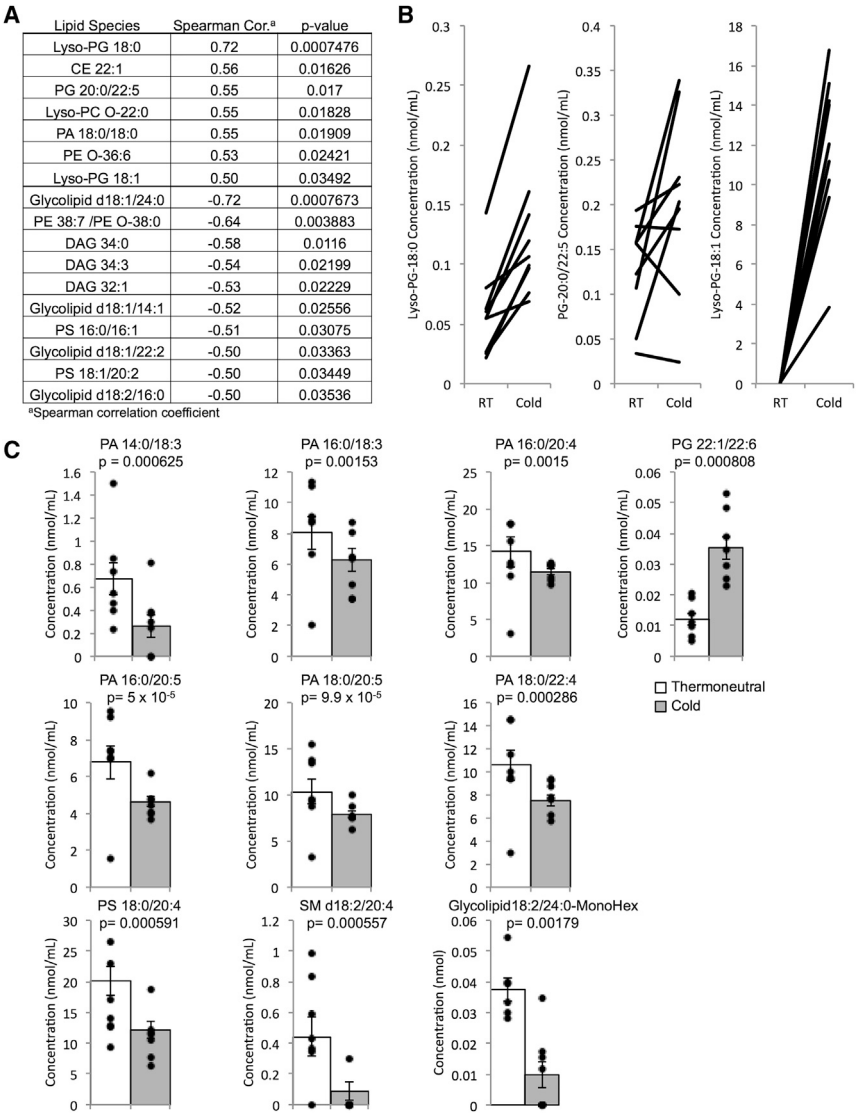

Figure 2. Phosphatidylglycerol Is a Biomarker of Human and Mouse BAT Activation

(A) Summary of plasma lipid species that were detectable in all human samples tested and that had a Spearman correlation coefficient greater than 0.5 or less than −0.5 with human BAT activity as measured by ^{18}fluorodeoxyglucose uptake at room temperature (RT) and 1 hr of mild cold exposure (14°C).

(B) Changes in plasma concentrations of 3 selected phosphatidylglycerol species by cold exposure compared to the concentrations at room temperature in individual human subjects. Plasma levels of these PGs were positively correlated with BAT activity, as described in (A). n = 9 paired plasma samples.

(C) Concentrations of the top 10 cold-regulated lipid species in mice. The lipids were selected according to Bonferroni-adjusted p value, comparing levels of circulating lipids in cold (5°C, 7 days) and thermoneutral (30°C, 7 days) groups. Data are presented as means ± SEM with values shown; n = 8 mice.

for the all the lipid classes profiled. (The viewer can be found at the URLs https://fiddle.jshell.net/mdlynes/2xrfs4e2/show/, https://fiddle.jshell.net/mdlynes/mwvu7p88/show/, and https://fiddle.jshell.net/mdlynes/66h3L44n/show/.)

Human BAT can be rapidly activated by mild cold exposure within 1 hr (Cypess et al., 2012); thus, we measured the plasma lipidome of nine subjects at room temperature (RT) and after a 1-hr cold exposure. Using our data viewer platform (https://fiddle.jshell.net/mdlynes/2xrfs4e2/show/), we were able to observe dynamic regulation of individual lipid species at cold versus room temperature conditions (higher significance is denoted by the larger circles in Figure 1B and in other similar types of dot plots presented in this paper). In spite of the fact that total lipid levels in each of the 17 lipid classes that we measured were not significantly changed by cold (Figure S1A), we detected significant changes in many low abundant individual lipid species (Figure 1B). For example, while total non-esterified fatty acid (NEFA) levels were found to be unaffected by a 1-hr cold challenge, as previously reported (Cypess et al., 2012), levels of certain individual FFAs were significantly altered. Specifically, although the most abundant FFAs, stearic acid (FFA 18:0) and oleic acid (FFA 18:1), were not changed by cold, there were, indeed, significant changes in several lipid species, such as FFA 22:6 and FFA 14:1 (Figures S1B and S1C). The online viewer that we created to further interrogate our lipidomics data allows high-resolution analysis of each of the lipid classes that we profiled. For most classes of lipids, the most abundant species were mostly unchanged by cold exposure, whereas more rare species could be either increased or decreased by alterations of environmental temperature.

We had access to blood samples from individuals that had also been scanned for BAT presence by positron emission tomography (PET) scan. To identify potential lipid biomarkers for BAT activation in humans, we performed correlation analysis between the plasma lipidome of each individual and the BAT activity levels estimated by ^{18}F-fluorodoxyglucose positron emission tomography (^{18}F-FDG PET), which is the gold standard. We excluded lipid species that were below the limit of detection in any individual and identified 10 lipid species that were negatively correlated with BAT activity and another 7 lipid species that positively correlated (Figure 2A). Notably, plasma levels of phosphatidylglycerol species—especially Lyso-PG 18:0; Lyso-PG 18:1; and, to a lesser extent, PG 20:0/22:5—were elevated upon cold exposure in

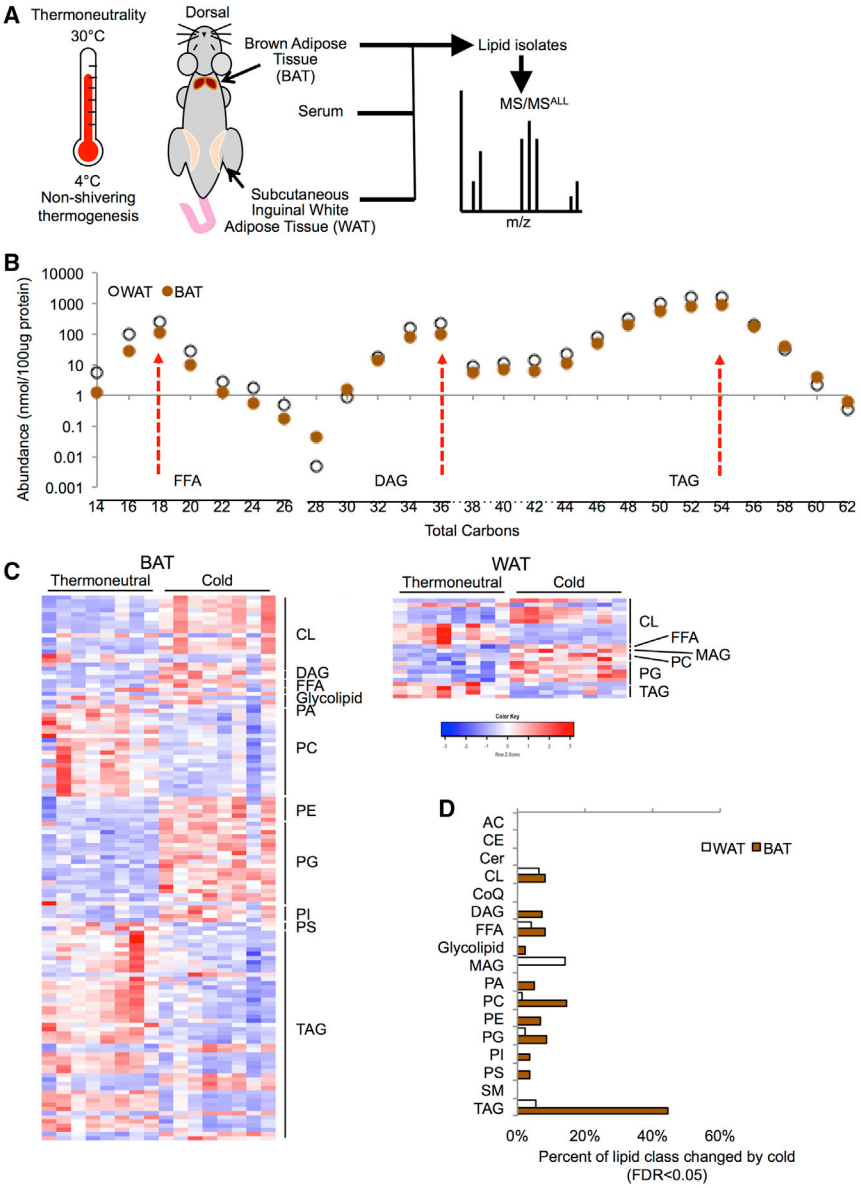

Figure 3. An MS/MS^{ALL}-Based Approach to Measure Thermogenically Regulated Lipid Content in Murine Adipose Tissue

(A) Mice housed in a diurnal incubator set to either thermoneutral or cold conditions, were sacrificed so that tissue and serum could be collected to measure lipid profiles using MS/MS^{ALL}.

(B) Total FFA, DAG, and TAG concentrations in BAT and WAT by total carbon number. Data are means for n = 8 per group.

(C) Heatmap showing the relative lipid concentrations of individual species that were significantly (FDR < 0.05 by Student's t test) changed by cold in BAT and WAT from mice housed in cold or thermoneutral conditions for 7 days. In these panels, each column represents one animal, while each row is a specific lipid species that was changed by cold. n = 8 per group.

(D) Percentage of lipid species in each class that were significantly (FDR < 0.05) regulated by cold exposure. The number of species that were either up- or downregulated was normalized to the number of species in each class that were considered for analysis.

these human subjects (Figure 2B; Figure S2). Although this cohort is relatively small, and these findings must be repeated in more subjects, lipid biomarkers for BAT activation could potentially supplant ^{18}F-FDG PET as a less expensive, safer alternative.

Recent studies in mice have demonstrated that carnitine-conjugated fatty acids were increased in circulation during thermogenesis to provide fuel to BAT (Simcox et al., 2017); however, we did not find any acyl-carnitine species that were significantly correlated with human BAT activation. This may be due to the acute cold-exposure paradigm used in our human studies, and future studies should include more chronic cold-exposure regimens. To extend our understanding to a mouse model of thermogenic activation, we housed mice for 7 days at either thermoneutral conditions (30°C) or cold (5°C) to induce non-shivering thermogenesis and performed lipidomic analyses on serum samples. We ranked lipids according to the Bonferroni-adjusted p value, comparing cold and thermoneutral conditions, and examined the top 10 species individually. Of these lipids, 9 lipid species were significantly decreased in circulation by cold exposure, including six PA species, one PS, and one SM (Figure 2C). We also detected one phosphatidylglycerol lipid species that was significantly increased in serum from animals housed in cold conditions (PG 22:1/22:6; Figure 2D). Though there was no overlap between the species identified in humans and mice, the difference in circulating phosphatidylglycerol species in cold humans and mice compared to controls supports a model wherein phosphatidylglycerol metabolism is activated by cold in mammals.

Comparative Lipidomic Response of BAT and WAT to Cold Exposure

To link changes in circulating lipids during thermogenesis with tissue metabolism, we analyzed the tissue lipidomics of BAT and WAT from mice housed in the cold compared to those of mice housed at thermoneutrality (Figure 3A; these data can also be accessed in our viewer at https://fiddle.jshell.net/mdlynes/mwvu7p88/show/ and https://fiddle.jshell.net/mdlynes/66h3L44n/show/). The distinct lipid profile of murine BAT and WAT has been previously documented (Hoene et al., 2014); however, the specific metabolic pathways that control lipid flux in situations of thermogenic demand are important in

understanding how to maximize thermogenesis in these tissues. In order to understand the network linking the regulation of specific lipids to physiologic metabolism, we first analyzed the data by probing individual lipid classes and then using the lipid viewer to get into detailed lipid maps.

Similar to what has been found in serum lipidomics, the total amount of most of the lipid classes was not significantly altered by cold exposure in BAT (Figure S3A) and WAT (Figure S3B). The FFA, DAG, and TAG contents of BAT and WAT have previously been reported to be distinct (Hoene et al., 2014), and these lipid families are major substrates for lipid oxidation. By analyzing the levels of FFA, DAG, and TAG at high resolution in adipose tissue, we observed three peaks in both BAT and WAT. These three most abundant types of FFA, DAG, and TAG are consistent with a high level of C18 fatty acid and the diacyl- and triacylglycerides with C18 fatty acid tails (C36, C54), which reflect the major fatty acids that make up these adipose depots (Figure 3B).

To further probe individual lipid species that were regulated by cold, we visualized all significantly changed lipid species using heatmaps. Using an FDR of 0.05 as a cutoff, a total of 130 species were significantly changed in BAT from cold-challenged animals, while 24 species were significantly regulated in WAT (Figure 3C). While cold exposure often had the same effect on lipids from the same class, there were clear examples of lipids that were regulated in the opposite direction of the majority of other species in the family. For example, most TAG species are decreased by cold in BAT; however, there are certain species that are increased by cold exposure.

By normalizing the number of lipids changed by cold exposure to the total number of lipids detected in each family, we showed enrichment of changes to TAG lipids, especially in BAT (Figure 3D). Similarly, cold exposure changed the concentration of approximately 10% of the lipid species in many phospholipid classes, which is consistent with reports of phospholipid metabolism being activated in adipose by cold (Marcher et al., 2015). PC, can activate systemic fatty acid catabolism (Liu et al., 2013); however, the classes with the most species upregulated by cold in BAT and WAT were cardiolipin and phosphatidylglycerol. Phosphatidylglycerol is a phospholipid precursor that is used to synthesize cardiolipin in cells in order to increase mitochondrial membrane production (Jiang et al., 2000). Interestingly, we found that a group of 15 cardiolipin species was regulated by cold in BAT (Figure S4A), and 11 cardiolipin species were regulated in WAT (Figure S4B), while there was no significant difference in total cardiolipin content in either tissue in cold-exposed animals. These data indicate a network of lipids that are regulated by cold in a tissue-specific manner and suggest that the lipid signature of phosphatidylglycerol in serum/plasma samples described earlier may be linked to activated phosphatidylglycerol/cardiolipin metabolism in adipose tissue.

Cardiolipin Synthesis Is Regulated by Thermogenesis

Cardiolipin is restricted to the mitochondrial membrane (Joshi et al., 2009; Ye et al., 2016); therefore, we hypothesized that increased cardiolipin biogenesis in thermogenic adipose tissue would coordinately increase phosphatidylglycerol lipid species and cardiolipin lipid species. We further examined the absolute concentration of individual phosphatidylglycerol species that are used to synthesize cardiolipin. In cells, phosphatidylglycerol can serve as a substrate for the enzyme CRLS1, which can catalyze the formation of cardiolipin from 1 phosphatidylglycerol molecule and 1 cytidine diphosphate DAG (CDP-DAG) molecule (Figure 4A). We calculated that approximately 15% of the total phosphatidylglycerol pool in both tissues was made up of phosphate groups with fatty acid tails 18:2, 18:1, 16:1, and 16:0. In mice housed in the cold for 7 days, there was a significant increase in phosphatidylglycerol species containing these fatty acid tails in BAT and WAT compared to thermoneutral controls (Figure 4B). As mentioned previously, the total level of cardiolipin was not different between mice in cold and thermoneutral conditions, due to small changes in the major constituent species of cardiolipin, specifically, CL 18:2/18:2/18:2/18:2. Importantly, when we compared other products of CRLS1 activity, specifically those containing phosphatidylglycerol species with 18:1, 16:1, and 16:0 fatty acid tails, the concentration of each was significantly higher in cold-challenged mice (Figure 4C). One limitation of the MS/MS^{ALL} approach that we took is the difficulty of quantifying different isomers, meaning that it is difficult to know whether the increased concentration of cardiolipin species with four 18-carbon chains and a total of six double bonds is due to changes in the concentration of CL 18:2/18:2/18:1/18:1 or CL 18:2/18:1/18:2/18:1 or both of these two isomers. For lipid species for which we have fatty acid composition listed, we designated the isomer molecular composition to identify the species. For phospholipids detected in the positive mode, where the head group was utilized and the fatty acid isomeric composition is more difficult to detect, we utilized the brutto nomenclature (Gao et al., 2017, 2018). Nevertheless, the data clearly indicated that cold exposure significantly increased the levels of multiple cardiolipin species in both BAT and WAT.

To determine whether cardiolipin synthesis in adipose tissue could be a marker of thermogenic activity, lipidomic profiling was performed on BAT and WAT from transgenic Myf5^{Cre}BMPr1a$^{fl/fl}$ knockout (KO) mice. As previously reported, the KO mice display a severe paucity of BAT, but they maintain normal body temperature through a compensatory increase in the recruitment of beige adipocytes in WAT (Schulz et al., 2013); therefore, these mice provide a unique model wherein beige adipogenesis is activated to compensate for the lack of interscapular BAT. We found that, even in thermoneutral conditions, several cardiolipin species were coordinately enriched in WAT from KO mice, compared to controls (Figure 5), suggesting that activation of cardiolipin biosynthesis by cold is not exclusive to BAT and also occurs in beige fat. Taken together, these data suggest that enhanced cardiolipin metabolism is a hallmark of thermogenic activation in adipose tissue.

DISCUSSION

In this study, we have generated data to extend our understanding of lipid metabolism during thermogenesis by leveraging the extreme sensitivity of MS/MS^{ALL} shotgun lipidomics. We have identified circulating lipid signatures of increased BAT activity in humans that includes increased metabolites involved in phosphatidylglycerol metabolism. In mice, phosphatidylglycerol metabolism is also regulated in the serum of mice housed in

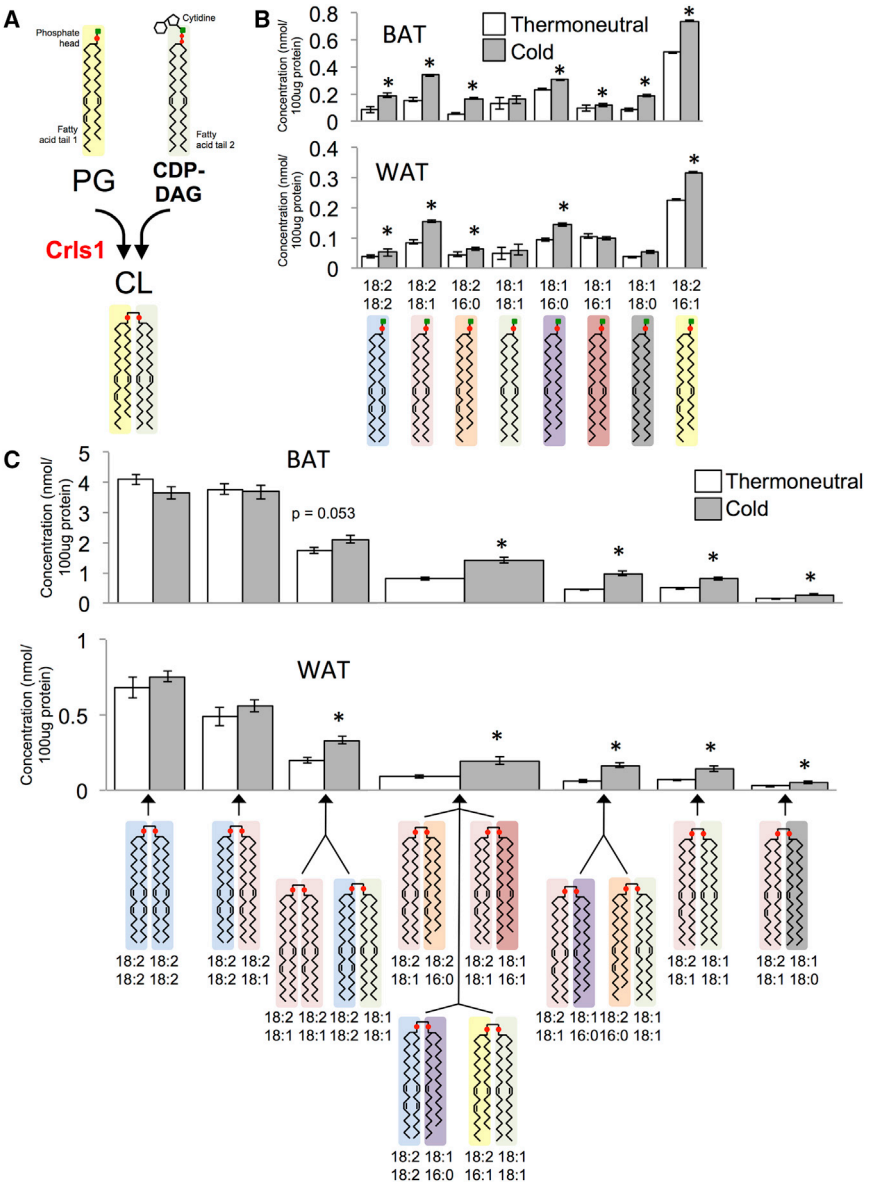

Figure 4. Phosphatidylglycerol and Cardiolipin Metabolism Is Activated in Cold Conditions

(A) Cardiolipin is synthesized from phosphatidylglycerol and CDP-DAG by the enzyme CRLS1.

(B) Concentrations of the 8 most abundant phosphatidylglycerol species in BAT and WAT from mice housed in thermoneutral or cold conditions for 7 days.

(C) Concentration of the most abundant cardiolipin species in BAT and WAT from mice housed in thermoneutral or cold conditions for 7 days. Data are presented as mean ± SEM; n = 8 per group. Asterisks denote statistically significant differences between groups by Student's t test (*$p < 0.05$).

cold conditions and is further enhanced in adipose tissue from animals housed in cold conditions. Although phospholipid metabolism has been implicated in adipose tissue thermogenesis (Marcher et al., 2015), our analysis shows that the downstream metabolite cardiolipin is the ultimate product of this increase in phospholipid metabolism. By studying a transgenic mouse model of enhanced beige adipocyte recruitment due to the severe paucity of BAT, we can further demonstrate that increased cardiolipin metabolism is a hallmark of thermogenic activation.

We have previously identified 12,13-diHOME, an oxidized metabolite of linoleic acid, as a lipid biomarker of thermogenic activation (Lynes et al., 2017). In the present study, we focus on non-oxidized structural lipid species dynamics during thermogenic activation and identify phosphatidylglycerol and cardiolipin metabolism as one of the key metabolic pathways regulated in thermogenic fat. Phospholipid metabolism has been reported to be activated in BAT by cold to support mitochondrial biogenesis (Marcher et al., 2015), and we find that species of phosphatidylglycerol were elevated in human and mouse circulation after cold challenge concomitant with increased cardiolipin species in the adipose tissue of mice housed at cold temperatures. In eukaryotes, cardiolipin is synthesized from phosphatidylglycerol and CDP-DAG exclusively in the mitochondria, where it constitutes up to 20% of total mitochondrial membrane lipid (Hostetler and van den Bosch, 1972). With four acyl chains and two negatively charged phosphate groups, cardiolipin has been called the "signature phospholipid" of the inner mitochondrial membrane and binds to a long list of membrane proteins, including respiratory complexes and the ADP-ATP carrier (Beyer and Klingenberg, 1985; Claypool et al., 2008; Eble et al., 1990; Lange et al., 2001; Palsdottir et al., 2003; Shinzawa-Itoh et al., 2007). CRLS1 overexpression in cardiac tissue improves the bioenergetics function of isolated mitochondria, potentially by increasing the ability of mitochondria to deal with increased energetic demands (Kiebish et al., 2012). Cardiolipin has been shown to bind directly to UCP1 and increase its stability in the mitochondrial membrane (Lee et al., 2015), and cardiolipin synthesis in brown and beige fat is essential for systemic energy homeostasis (Sustarsic et al., 2018).

We have shown that cardiolipin metabolism is enhanced in the setting of thermogenesis and that in mice, BAT and WAT enhance cardiolipin metabolism by increasing concentrations of several phosphatidylglycerol substrates. Interestingly, specific phosphatidylglycerol and cardiolipin species are increased by cold, suggesting that mitochondrial biogenesis may rely preferentially on these species.

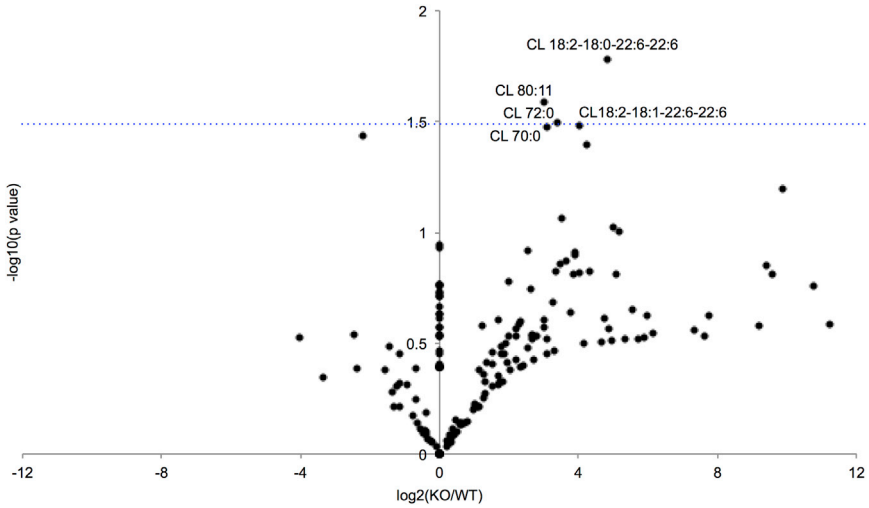

Figure 5. Cardiolipin Metabolism Is Activated in WAT in a Mouse Model of Browning

Volcano plot of all cardiolipin species measured by MS/MS^{ALL} in sera of Myf5^{Cre}BMPr1a$^{fl/fl}$ mice (KO) compared to control (WT) mice displayed as the log base-2 ratio of KO to wild-type (WT) mouse conditions versus the inverse log base-10 of the p value of this comparison (Student's two-tailed t test). The dotted blue line indicates an approximate nominal p value of 0.05. n = 4–5 per group.

We observed no difference in the tissue concentration of the most abundant cardiolipin species, CL 18:2/18:2/18:2/18:2, in BAT or WAT from animals housed in cold or in WAT from Myf5-^{Cre}BMPr1a$^{fl/fl}$ mice. CL 18:2/18:2/18:2/18:2 has four C18:2 acyl chains and has been shown to constitute approximately 50% of all cardiolipin in heart and liver (Pangborn, 1947); however, increased CRLS1 expression in cold-exposed animals was correlated with increased concentrations of phosphatidylglycerol substrates and cardiolipin metabolites containing C18:1, C16:1 and C16:0 acyl chains. Our data are consistent with a model wherein cold activates the anabolism of nascent cardiolipin molecules that can be subsequently remodeled by the deacylation-reacylation cycle.

Thermogenic fat is present in humans (Cypess et al., 2009; van Marken Lichtenbelt et al., 2009; Virtanen et al., 2009), and recent studies have demonstrated that cold-exposure regimens can improve insulin sensitivity and glucose tolerance (Hanssen et al., 2015); however, the effects of cold on lipid metabolism in humans are less clear. To maximize the therapeutic potential of thermogenic fat in humans, it is critical to understand the metabolites that are consumed by this tissue when it is activated. Because our lipidomic profiling in humans was limited to plasma samples, we are unable to determine which tissues are secreting or taking up the lipid species that were detected. Though our study did have the advantage of paired before-and-after cold treatment samples, it is still difficult to tease apart whether the changes in plasma lipids are the result of catabolism or anabolism. Further studies are needed to determine the specific lipid metabolic pathways activated in human BAT tissue. In lieu of human tissue, in the present study, we have attempted to match the lipidomic profile of human plasma during cold challenge with lipid profiles of murine serum and adipose tissue. Due to the limited access to human BAT, human adipocytes derived from *in vitro* differentiation of immortalized cell lines (Xue et al., 2015) could be used to measure lipid dynamics of an *in vitro* model of human tissue.

An understanding of the dynamics of lipid metabolism in thermogenic adipose tissue is key to formulating strategies to enhance activity as a treatment for obesity and its sequelae. Since brown and beige fat activity is elevated by cold, the data from the present study could be used to generate panels of biomarkers for thermogenic fat activation. By designing targeted approaches to measure circulating lipid species like the phosphatidylglycerol species that we identified, it may be possible to measure BAT activity while avoiding the drawbacks and expense of using radioactive tracers. The data reported here provide an exciting opportunity to understand lipid metabolism and regulatory mechanisms that are associated with thermogenically competent tissue.

EXPERIMENTAL PROCEDURES

Human Subjects

Human plasma was acquired from a previously performed cold-exposure experiment (Cypess et al., 2012). Briefly, healthy volunteers participated in three separate, independent study visits conducted in random order based on a Latin Square design. The night before the study day, they were admitted to the clinical research center and began fasting from 12:00 a.m. onward. Room temperature was maintained above 23°C throughout the stay in the clinical research center. Upon waking the next morning, the volunteers put on a standard hospital scrub suit. Depending on the study day, one of three stimuli was given: the volunteer received a single intramuscular dose of ephedrine, 1 mg/kg, or an equal volume of saline; or the volunteer was transported to a room set to 20°C and donned a surgeon's cooling vest (Polar Products) with the water temperature set to 14°C, which was monitored by a digital thermometer (Fisher Scientific). Sixty minutes after the injection of ephedrine or saline, or the initiation of cold exposure, blood was drawn for measurement of lipid levels, and then an intravenous bolus of 440 MBq (12 mCi) of ^{18}F-FDG was administered. Sixty minutes after ^{18}F-FDG injection, images were acquired using a Discovery LS multidetector helical PET-CT (computed tomography) scanner (GE Medical Systems). BAT mass and activity were quantified using the PET-CT Viewer shareware.

Mice

All animal procedures were approved by the Institutional Animal Use and Care Committee at Joslin Diabetes Center. For the cold-exposure experiments, 12-week-old male C57BL/6J mice (stock no. 000664) were purchased from The Jackson Laboratory. Alternatively, transgenic mice carrying floxed alleles for the bone morphogenetic protein (BMP) receptor 1A were used to generate conditional gene-deletion mouse models by intercrossing with *Myf5*-driven Cre recombinase and were compared to Cre-negative littermate controls, as described previously (Schulz et al., 2013). In addition to C57BL/6J mice, these transgenic animals were used for all chronic cold-exposure experiments, with mice 10–18 weeks of age housed in a temperature-controlled diurnal incubator (Caron Products & Services) at either 4°C (cold) or 30°C (thermoneutrality) on a 12-hr:12-hr light:dark cycle. In all experiments, interscapular BAT, inguinal WAT, and serum were dissected after sacrifice.

Lipidomic Profiling

Human plasma samples were thawed on ice. Before extraction, a designated cocktail of internal standards was added to 25 μL plasma. 4 mL chloroform:methanol (1:1, v/v) was added to each sample, and the lipid extraction was performed as previously described (Kiebish et al., 2010; Rockwell et al., 2016). Lipid extraction was automated using a customized sequence on a Hamilton Robobtics STARlet system (Hamilton, Reno, NV, USA) to meet the high-throughput requirements. Lipid extracts were dried under nitrogen and reconstituted in 68 μL chloroform:methanol (1:1, v/v). Samples were flushed with nitrogen and stored at −20°C.

For tissue analysis, 10–20 mg mouse adipose tissue was transferred to an OMNI bead tube with 0.5 mL cold MeOH (−20°C) and was homogenized for 1.5 min at 4°C using the OMNI Cryo Bead Ruptor 24 (OMNI International, Kennesaw, GA, USA). An aliquot of the homogenate was taken for the protein analysis using a bicinchoninic acid (BCA) assay, and 1 mg of the sample based on protein concentration was added to internal standards and 4 mL chloroform:methanol (1:1, v/v) for the extraction. Lipid extracts were dried under nitrogen and reconstituted in 400 μL chloroform:methanol (1:1, v/v). Samples were flushed with nitrogen and stored at −20°C.

The concentrated sample was diluted 50× in isopropanol:methanol:acetonitrile:H_2O (3:3:3:1, by volume) with 2 mM ammonium acetate. The delivery of the solution to the SCIEX TripleTOF 5600+ (Sciex, Framingham, MA, USA) was carried out using an Ekspert MicroLC 200 system with a flow rate at 6 μL/min on a customized loop. The parameters of the mass spectrometer were optimized, and the samples were analyzed automatically using a data-independent analysis strategy, allowing for MS/MS^{ALL} high resolution and high mass accuracy (Simons et al., 2012).

Statistics

All statistics were calculated using Microsoft Excel, GraphPad Prism and RStudio. For the online viewer, we provide the FDR for the comparison of lipidomics in mouse tissue, and for lipidomics of the human plasma, we used Bonferroni-adjusted p value. All comparisons of lipid species within a family were considered post hoc analyses. In all cases, we assumed equal variance. For consistency, the Spearman correlation coefficient is shown; however, all Pearson and Kendall coefficients reached similar levels of significance. No statistical method was used to predetermine sample size. The experiments were not randomized or blinded.

SUPPLEMENTAL INFORMATION

Supplemental Information includes four figures and three tables and can be found with this article online at https://doi.org/10.1016/j.celrep.2018.06.073.

ACKNOWLEDGMENTS

This work was supported in part by U.S. NIH grants R01DK077097 and R01DK102898 (to Y.-H.T.) and by grant P30DK036836 (to Joslin Diabetes Center's Diabetes Research Center; DRC) from the National Institute of Diabetes and Digestive and Kidney Diseases. M.D.L. was supported by NIH grants T32DK007260, F32DK102320, and K01DK111714. We thank H. Pan in the Joslin Bioinformatics Core. This manuscript is dedicated to the memory of Sean Peters.

AUTHOR CONTRIBUTIONS

M.D.L. designed and directed research, carried out experiments, analyzed data, and wrote the paper. F.S., E.G.S., and Z.G.-H. designed research and edited the paper. L.O.L., C.-H.W., S.-C.S., and T.L.H. carried out *in vitro* assays. F.G., N.R.N., and M.A.K. oversaw lipidomics experiments. E.Y.C. performed lipidomic experiments and analyzed data. T.J.S. performed experiments with the Myf5^{Cre}BMPr1a$^{fl/fl}$ mice. A.M.C. designed research and carried out human cold-exposure experiments. Y.-H.T. directed the research and co-wrote the paper.

DECLARATION OF INTERESTS

The authors declare the following competing interests: M.A.K., E.Y.C., N.R.N., and F.G. are employees of BERG.

Received: September 27, 2017
Revised: May 7, 2018
Accepted: June 15, 2018
Published: July 17, 2018

REFERENCES

Bartelt, A., Bruns, O.T., Reimer, R., Hohenberg, H., Ittrich, H., Peldschus, K., Kaul, M.G., Tromsdorf, U.I., Weller, H., Waurisch, C., et al. (2011). Brown adipose tissue activity controls triglyceride clearance. Nat. Med. *17*, 200–205.

Bartelt, A., John, C., Schaltenberg, N., Berbée, J.F.P., Worthmann, A., Cherradi, M.L., Schlein, C., Piepenburg, J., Boon, M.R., Rinninger, F., et al. (2017). Thermogenic adipocytes promote HDL turnover and reverse cholesterol transport. Nat. Commun. *8*, 15010.

Berbée, J.F., Boon, M.R., Khedoe, P.P., Bartelt, A., Schlein, C., Worthmann, A., Kooijman, S., Hoeke, G., Mol, I.M., John, C., et al. (2015). Brown fat activation reduces hypercholesterolaemia and protects from atherosclerosis development. Nat. Commun. *6*, 6356.

Beyer, K., and Klingenberg, M. (1985). ADP/ATP carrier protein from beef heart mitochondria has high amounts of tightly bound cardiolipin, as revealed by 31P nuclear magnetic resonance. Biochemistry *24*, 3821–3826.

Blondin, D.P., Labbé, S.M., Phoenix, S., Guérin, B., Turcotte, E.E., Richard, D., Carpentier, A.C., and Haman, F. (2015). Contributions of white and brown adipose tissues and skeletal muscles to acute cold-induced metabolic responses in healthy men. J. Physiol. *594*, 701–714.

Cannon, B., Shabalina, I.G., Kramarova, T.V., Petrovic, N., and Nedergaard, J. (2006). Uncoupling proteins: a role in protection against reactive oxygen species–or not? Biochim. Biophys. Acta *1757*, 449–458.

Chondronikola, M., Volpi, E., Børsheim, E., Porter, C., Annamalai, P., Enerbäck, S., Lidell, M.E., Saraf, M.K., Labbe, S.M., Hurren, N.M., et al. (2014). Brown adipose tissue improves whole-body glucose homeostasis and insulin sensitivity in humans. Diabetes *63*, 4089–4099.

Cinti, S. (2017). UCP1 protein: The molecular hub of adipose organ plasticity. Biochimie *134*, 71–76.

Claypool, S.M., Oktay, Y., Boontheung, P., Loo, J.A., and Koehler, C.M. (2008). Cardiolipin defines the interactome of the major ADP/ATP carrier protein of the mitochondrial inner membrane. J. Cell Biol. *182*, 937–950.

Cooney, G.J., Caterson, I.D., and Newsholme, E.A. (1985). The effect of insulin and noradrenaline on the uptake of 2-[1-14C]deoxyglucose in vivo by brown adipose tissue and other glucose-utilising tissues of the mouse. FEBS Lett. *188*, 257–261.

Cypess, A.M., Lehman, S., Williams, G., Tal, I., Rodman, D., Goldfine, A.B., Kuo, F.C., Palmer, E.L., Tseng, Y.H., Doria, A., et al. (2009). Identification and importance of brown adipose tissue in adult humans. N. Engl. J. Med. *360*, 1509–1517.

Cypess, A.M., Chen, Y.C., Sze, C., Wang, K., English, J., Chan, O., Holman, A.R., Tal, I., Palmer, M.R., Kolodny, G.M., and Kahn, C.R. (2012). Cold but not sympathomimetics activates human brown adipose tissue in vivo. Proc. Natl. Acad. Sci. USA *109*, 10001–10005.

Eble, K.S., Coleman, W.B., Hantgan, R.R., and Cunningham, C.C. (1990). Tightly associated cardiolipin in the bovine heart mitochondrial ATP synthase as analyzed by 31P nuclear magnetic resonance spectroscopy. J. Biol. Chem. *265*, 19434–19440.

Gao, F., McDaniel, J., Chen, E.Y., Rockwell, H.E., Drolet, J., Vishnudas, V.K., Tolstikov, V., Sarangarajan, R., Narain, N.R., and Kiebish, M.A. (2017). Dynamic and temporal assessment of human dried blood spot MS/MS^{ALL} shotgun lipidomics analysis. Nutr. Metab. (Lond.) *14*, 28.

Gao, F., McDaniel, J., Chen, E.Y., Rockwell, H.E., Nguyen, C., Lynes, M.D., Tseng, Y.H., Sarangarajan, R., Narain, N.R., and Kiebish, M.A. (2018). Adapted MS/MS^{ALL} shotgun lipidomics approach for analysis of cardiolipin molecular species. Lipids *53*, 133–142.

Haemmerle, G., Lass, A., Zimmermann, R., Gorkiewicz, G., Meyer, C., Rozman, J., Heldmaier, G., Maier, R., Theussl, C., Eder, S., et al. (2006). Defective lipolysis and altered energy metabolism in mice lacking adipose triglyceride lipase. Science *312*, 734–737.

Hanssen, M.J., Hoeks, J., Brans, B., van der Lans, A.A., Schaart, G., van den Driessche, J.J., Jörgensen, J.A., Boekschoten, M.V., Hesselink, M.K., Havekes, B., et al. (2015). Short-term cold acclimation improves insulin sensitivity in patients with type 2 diabetes mellitus. Nat. Med. *21*, 863–865.

Hoene, M., Li, J., Häring, H.U., Weigert, C., Xu, G., and Lehmann, R. (2014). The lipid profile of brown adipose tissue is sex-specific in mice. Biochim. Biophys. Acta *1842*, 1563–1570.

Hostetler, K.Y., and van den Bosch, H. (1972). Subcellular and submitochondrial localization of the biosynthesis of cardiolipin and related phospholipids in rat liver. Biochim. Biophys. Acta *260*, 380–386.

Jiang, F., Ryan, M.T., Schlame, M., Zhao, M., Gu, Z., Klingenberg, M., Pfanner, N., and Greenberg, M.L. (2000). Absence of cardiolipin in the crd1 null mutant results in decreased mitochondrial membrane potential and reduced mitochondrial function. J. Biol. Chem. *275*, 22387–22394.

Joshi, A.S., Zhou, J., Gohil, V.M., Chen, S., and Greenberg, M.L. (2009). Cellular functions of cardiolipin in yeast. Biochim. Biophys. Acta *1793*, 212–218.

Kazak, L., Chouchani, E.T., Jedrychowski, M.P., Erickson, B.K., Shinoda, K., Cohen, P., Vetrivelan, R., Lu, G.Z., Laznik-Bogoslavski, D., Hasenfuss, S.C., et al. (2015). A creatine-driven substrate cycle enhances energy expenditure and thermogenesis in beige fat. Cell *163*, 643–655.

Kiebish, M.A., Bell, R., Yang, K., Phan, T., Zhao, Z., Ames, W., Seyfried, T.N., Gross, R.W., Chuang, J.H., and Han, X. (2010). Dynamic simulation of cardiolipin remodeling: greasing the wheels for an interpretative approach to lipidomics. J. Lipid Res. *51*, 2153–2170.

Kiebish, M.A., Yang, K., Sims, H.F., Jenkins, C.M., Liu, X., Mancuso, D.J., Zhao, Z., Guan, S., Abendschein, D.R., Han, X., and Gross, R.W. (2012). Myocardial regulation of lipidomic flux by cardiolipin synthase: setting the beat for bioenergetic efficiency. J. Biol. Chem. *287*, 25086–25097.

Lange, C., Nett, J.H., Trumpower, B.L., and Hunte, C. (2001). Specific roles of protein-phospholipid interactions in the yeast cytochrome bc1 complex structure. EMBO J. *20*, 6591–6600.

Lee, Y., Willers, C., Kunji, E.R., and Crichton, P.G. (2015). Uncoupling protein 1 binds one nucleotide per monomer and is stabilized by tightly bound cardiolipin. Proc. Natl. Acad. Sci. USA *112*, 6973–6978.

Liu, S., Brown, J.D., Stanya, K.J., Homan, E., Leidl, M., Inouye, K., Bhargava, P., Gangl, M.R., Dai, L., Hatano, B., et al. (2013). A diurnal serum lipid integrates hepatic lipogenesis and peripheral fatty acid use. Nature *502*, 550–554.

Lu, X., Solmonson, A., Lodi, A., Nowinski, S.M., Sentandreu, E., Riley, C.L., Mills, E.M., and Tiziani, S. (2017). The early metabolomic response of adipose tissue during acute cold exposure in mice. Sci. Rep. *7*, 3455.

Lynes, M.D., and Tseng, Y.H. (2015). The thermogenic circuit: regulators of thermogenic competency and differentiation. Genes Dis. *2*, 164–172.

Lynes, M.D., and Tseng, Y.H. (2018). Deciphering adipose tissue heterogeneity. Ann. N Y Acad. Sci. *1411*, 5–20.

Lynes, M.D., Leiria, L.O., Lundh, M., Bartelt, A., Shamsi, F., Huang, T.L., Takahashi, H., Hirshman, M.F., Schlein, C., Lee, A., et al. (2017). The cold-induced lipokine 12,13-diHOME promotes fatty acid transport into brown adipose tissue. Nat Med. *23*, 631–637.

Marcher, A.B., Loft, A., Nielsen, R., Vihervaara, T., Madsen, J.G., Sysi-Aho, M., Ekroos, K., and Mandrup, S. (2015). RNA-seq and mass-spectrometry-based lipidomics reveal extensive changes of glycerolipid pathways in brown adipose tissue in response to cold. Cell Rep. *13*, 2000–2013.

Ogawa, K., Ohno, T., and Kuroshima, A. (1987). Muscle and brown adipose tissue fatty acid profiles in cold-exposed rats. Jpn. J. Physiol. *37*, 783–796.

Orava, J., Nuutila, P., Lidell, M.E., Oikonen, V., Noponen, T., Viljanen, T., Scheinin, M., Taittonen, M., Niemi, T., Enerbäck, S., and Virtanen, K.A. (2011). Different metabolic responses of human brown adipose tissue to activation by cold and insulin. Cell Metab. *14*, 272–279.

Palsdottir, H., Lojero, C.G., Trumpower, B.L., and Hunte, C. (2003). Structure of the yeast cytochrome bc1 complex with a hydroxyquinone anion Qo site inhibitor bound. J. Biol. Chem. *278*, 31303–31311.

Pangborn, M.C. (1947). The composition of cardiolipin. J. Biol. Chem. *168*, 351–361.

Petrovic, N., Walden, T.B., Shabalina, I.G., Timmons, J.A., Cannon, B., and Nedergaard, J. (2010). Chronic peroxisome proliferator-activated receptor gamma (PPARgamma) activation of epididymally derived white adipocyte cultures reveals a population of thermogenically competent, UCP1-containing adipocytes molecularly distinct from classic brown adipocytes. J. Biol. Chem. *285*, 7153–7164.

Ricquier, D., Mory, G., Nechad, M., and Hémon, P. (1978). Effects of cold adaptation and re-adaptation upon the mitochondrial phospholipids of brown adipose tissue. J. Physiol. (Paris) *74*, 695–702.

Rockwell, H.E., Gao, F., Chen, E.Y., McDaniel, J., Sarangarajan, R., Narain, N.R., and Kiebish, M.A. (2016). Dynamic assessment of functional lipidomic analysis in human urine. Lipids *51*, 875–886.

Schreiber, R., Diwoky, C., Schoiswohl, G., Feiler, U., Wongsiriroj, N., Abdellatif, M., Kolb, D., Hoeks, J., Kershaw, E.E., Sedej, S., et al. (2017). Cold-induced thermogenesis depends on ATGL-mediated lipolysis in cardiac muscle, but not brown adipose tissue. Cell Metab. *26*, 753–763.e7.

Schulz, T.J., Huang, P., Huang, T.L., Xue, R., McDougall, L.E., Townsend, K.L., Cypess, A.M., Mishina, Y., Gussoni, E., and Tseng, Y.H. (2013). Brown-fat paucity due to impaired BMP signalling induces compensatory browning of white fat. Nature *495*, 379–383.

Seale, P., Kajimura, S., and Spiegelman, B.M. (2009). Transcriptional control of brown adipocyte development and physiological function–of mice and men. Genes Dev. *23*, 788–797.

Shinzawa-Itoh, K., Aoyama, H., Muramoto, K., Terada, H., Kurauchi, T., Tadehara, Y., Yamasaki, A., Sugimura, T., Kurono, S., Tsujimoto, K., et al. (2007). Structures and physiological roles of 13 integral lipids of bovine heart cytochrome c oxidase. EMBO J. *26*, 1713–1725.

Simcox, J., Geoghegan, G., Maschek, J.A., Bensard, C.L., Pasquali, M., Miao, R., Lee, S., Jiang, L., Huck, I., Kershaw, E.E., et al. (2017). Global analysis of plasma lipids identifies liver-derived acylcarnitines as a fuel source for brown fat thermogenesis. Cell Metab. *26*, 509–522.e6.

Simons, B., Kauhanen, D., Sylvänne, T., Tarasov, K., Duchoslav, E., and Ekroos, K. (2012). Shotgun lipidomics by sequential precursor ion fragmentation on a hybrid quadrupole time-of-flight mass spectrometer. Metabolites *2*, 195–213.

Strunecká, A., Olivierusová, L., Kubista, V., and Drahota, Z. (1981). Effect of cold stress and norepinephrine on the turnover of phospholipids in brown adipose tissue of the golden hamster (*Mesocricetus auratus*). Physiol. Bohemoslov. *30*, 307–313.

Sustarsic, E.G., Ma, T., Lynes, M.D., Larsen, M., Karavaeva, I., Havelund, J.F., Nielsen, C.H., Jedrychowski, M.P., Moreno-Torres, M., Lundh, M., et al. (2018). Cardiolipin synthesis in brown and beige fat mitochondria is essential for systemic energy homeostasis. Cell Metab. Published May 18, 2018. https://doi.org/10.1016/j.cmet.2018.05.003.

van Marken Lichtenbelt, W.D., Vanhommerig, J.W., Smulders, N.M., Drossaerts, J.M., Kemerink, G.J., Bouvy, N.D., Schrauwen, P., and Teule, G.J. (2009). Cold-activated brown adipose tissue in healthy men. N. Engl. J. Med. *360*, 1500–1508.

Virtanen, K.A., Lidell, M.E., Orava, J., Heglind, M., Westergren, R., Niemi, T., Taittonen, M., Laine, J., Savisto, N.J., Enerbäck, S., and Nuutila, P. (2009). Functional brown adipose tissue in healthy adults. N. Engl. J. Med. *360*, 1518–1525.

Wu, J., Boström, P., Sparks, L.M., Ye, L., Choi, J.H., Giang, A.H., Khandekar, M., Virtanen, K.A., Nuutila, P., Schaart, G., et al. (2012). Beige adipocytes are a distinct type of thermogenic fat cell in mouse and human. Cell *150*, 366–376.

Xue, R., Lynes, M.D., Dreyfuss, J.M., Shamsi, F., Schulz, T.J., Zhang, H., Huang, T.L., Townsend, K.L., Li, Y., Takahashi, H., et al. (2015). Clonal analyses and gene profiling identify genetic biomarkers of the thermogenic potential of human brown and white preadipocytes. Nat. Med. *21*, 760–768.

Ye, C., Shen, Z., and Greenberg, M.L. (2016). Cardiolipin remodeling: a regulatory hub for modulating cardiolipin metabolism and function. J. Bioenerg. Biomembr. *48*, 113–123.